ACS Medicinal Chemistry Letters

Letter

Discovery of Selective, Covalent FGFR4 Inhibitors with Anti-tumor Activity in Models of Hepato-cellular Carcinoma

Haibo Liu, Deqiang niu, Robert Tjin Tham Sjin, Alex Dubrovskiy, Zhendong Zhu, Joseph J. McDonald, Kelly Fahnoe, Zhigang Wang, Mark Munson, Andrew Scholte, Matthieu Barrague, Maria Fitzgerald, Jinyu Liu, Michael Kothe, Fangxian Sun, Joshua Murtie, Jie Ge, Jennifer Rocnik, Darren Harvey, Beatriz Ospina, Keli Perron, Gang Zheng, Elvis Shehu, and Laura Akullian D'Agostino

ACS Med. Chem. Lett., **Just Accepted Manuscript** • DOI: 10.1021/acsmedchemlett.9b00601 • Publication Date (Web): 06 Mar 2020

Discovery of Selective, Covalent FGFR4 Inhibitors with Anti-tumor Activity in Models of Hepatocellular Carcinoma

Haibo Liu†, Deqiang Niu†, Robert Tjin Tham Sjin†, Alex Dubrovskiy†, Zhendong Zhu†, Joseph J McDonald†, Kelly Fahnoe†, Zhigang Wang†, Mark Munson‡, Andrew Scholte‡, Matthieu Barrague‡, Maria Fitzgerald‡, Jinyu Liu‡, Michael Kothe‡, Fangxian Sun‡, Joshua Murtie‡, Jie Ge‡, Jennifer Rocnik‡, Darren Harvey‡, Beatriz Ospina‡, Keli Perron‡, Gang Zheng‡, Elvis Shehu‡, Laura Akullian D'Agostino†

†Departments of Chemistry, Biology, and Biochemistry, Bristol-Myers Squibb, 200 Cambridge Park Dr., Cambridge, MA 02140;

‡Departments of Chemistry, Biology, DMPK, Structural Biology, and Pharmacology, Sanofi, 153 Second Ave., Waltham, MA 02451

KEYWORDS. Selective FGFR4 inhibition, kinase inhibitor, targeted covalent inhibitor, hepatocellular carcinoma

ABSTRACT: Hepatocellular carcinoma (HCC) accounts for 85–90% of primary liver cancer and is one of the most common forms of cancer worldwide.[1] Aberrant signaling of the FGF19-FGFR4 pathway has been shown to cause HCC in mice and is hypothesized to be a driver in FGF19 amplified HCC in humans.[2] Multiple small molecule inhibitors have been pursued as targeted therapies for HCC in recent years including several selective FGFR4 inhibitors that are currently being evaluated in clinical trials. Herein we report a novel series of highly selective, covalent 2-amino-6, 8-dimethyl-pyrido[2,3-d]pyrimidin-7(8H)-ones that potently and selectively inhibit FGFR4 signaling through covalent modification of Cys552, which was confirmed by X-ray crystallography. Correlative PK/PD and tumor regression were observed in preclinical models of orthotopic and sorafenib-resistant HCC.

Hepatocellular carcinoma (HCC) accounts for 85-90% of primary liver cancer and is one of the most common forms of cancer with the highest rate of cancer-related mortality worldwide.[1] Pathogenically, the causes for HCC have been commonly associated with chronic liver stress such as viral infection, metabolic disorders, or alcohol abuse. In 2018, there were 841,000 incidents of liver cancer and 781,000 deaths worldwide.[2] In 2017, in the US alone, there were approximately 40,000 cases diagnosed and 29,000 deaths.[3] The current standard of care for HCC is the multikinase inhibitor sorafenib which was approved in 2007 based on a three month improvement in median survival and time to progression.[4] A significant number of patients present intrinsic resistance to sorafenib treatment and still many others develop acquired resistance.[5] In 2017, two second line therapies were approved: multikinase inhibitor regorafenib in Japan and the EU, and anti-PD1 immunotherapy nivolumab in the US. Notwithstanding these notable successes, and despite many phase 3 attempts to treat HCC, there remains a significant shortage of therapeutic options.[6]

The fibroblast growth factor receptors (FGFRs) are a family of transmembrane receptor tyrosine kinases comprised of FGFR1, 2, 3, and 4 that interact with 18 different fibroblast growth factor (FGF) ligands. FGF/FGFR signaling pathways play essential roles in embryogenesis, metabolism, and tissue homeostasis. Aberrant FGF/FGFR signaling has been implicated in lung cancer, breast cancer, gastric cancer, and HCC among others.[7] FGFR4 is the predominant isoform expressed in human hepatocytes and FGF19 is the primary, albeit not exclusive, ligand for FGFR4. FGFR4 pathway activation requires FGF19 binding as well as the tissue-resident cofactor β-klotho (KLB). The combination of FGF19/FGFR4/KLB is uniquely effective in driving hepatocyte proliferation, dysplasia, and neoplasia. These effects can be reversed *in vitro* and in animal models via neutralization of FGF19 and/or inhibition of FGFR4, supporting the hypothesis that inhibition of FGFR4 signaling may provide therapeutic benefit in certain cancers.[8-10] Furthermore, through selective inhibition of FGFR4 over FGFR 1–3, one could achieve therapeutic benefit without encountering dose limiting toxicities associated with inhibition of FGFR1 and FGFR3, particularly hyperphosphatemia and hypocalcemia. Taken together, these data collectively support the therapeutic rationale for selective inhibition of FGFR4 in patients with FGF19 amplified HCC.

FGFR proteins are highly homologous with sequence similarity of 88% on average and sequence homology of 68%. When our program was initiated, only pan-FGFR inhibitors were known and often exhibited weaker potency against FGFR4 compared to FGFRs 1–3. Examples include PD173074, BGJ-398 and AZD4547 (Figure 1). In recent years, the discovery of potent and selective FGFR4 inhibitors has been actively pursued by numerous groups and has been the topic of multiple reviews.[11] A diverse set of small molecule inhibitors has been identified (Figure 1) including several that are currently being evaluated in clinical trials (BLU554, H3B-6527

and FGF401). In a recent Phase 1 study, BLU-554 was shown to elicit clinical responses in patients with advanced FGF19 positive HCC.[12] Herein, we report the design, synthesis and biological evaluation of a novel series of potent and selective 2-amino-6-methylpyrido[2,3-d]pyrimidin-7(8H)-one FGFR4 inhibitors that promote tumor regression in sorafenib-resistant and orthotopic human tumor xenograft models.

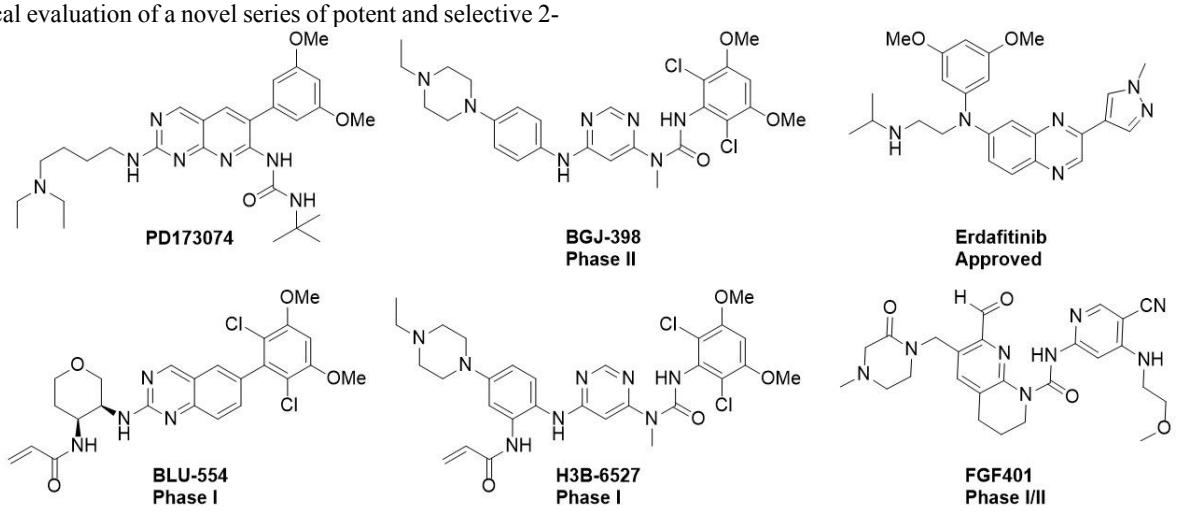

Figure 1. Structures of representative pan-FGFR and selective FGFR4 inhibitors.

Covalent drugs have proven successful as targeted therapies for a variety of malignancies with known oncogenic drivers, achieving high levels of target engagement and protracted target occupancy *in vivo*. In addition, covalent inhibition may provide an advantage in cases of acquired drug resistance.[1,3] FGFR4 contains a unique cysteine (Cys) residue numbered 552. FGFRs 1–3 present a tyrosine (Tyr) at this position. Furthermore, Cys552 is conserved in just 10 human protein kinases including MK2, MK3, S6K2, STK40 and TTK. Thus, covalently targeting the Cys552 in FGFR4 is an appealing strategy for achieving selective inhibition of FGFR4 both with respect to isoform and kinome selectivity, as well as addressing challenges related to acquired resistance.

Through structure-based design, we were able to identify an ATP competitive 2-amino-6, 8-dimethylpyrido[2,3-d]pyrimidin-7(8H)-one scaffold that achieved covalent modification of Cys552 and inhibition of the catalytic activity of FGFR4. Optimization of cellular potency, selectivity, and pharmacokinetic properties resulted in identification of compound **1** which inhibits pFGFR4 signaling in cells with IC_{50} = 9 nM and >100 fold selectivity over FGFRs 1–3. FGFR2 was used as a surrogate marker of FGFR 1–3 activity in cells as potency against FGFRs 1–3 was generally similar.

A co-crystal structure of compound **1** covalently bound to the kinase domain of human FGFR4 was determined by X-ray crystallography at 1.9 Å resolution (Figure 2, PDB 6V9C). The structure shows that compound **1** binds to the DFG-in conformation of the FGFR4 kinase domain. The acrylamide forms a covalent bond with Cys552 in the hinge region of the protein. Additionally, the acrylamide forms hydrogen bonding interactions with Ala553 in the hinge region and Arg483 located on the N lobe. The carbonyl of the pyridopyrimidinone core forms a water mediated hydrogen bond with Asp630 near the DFG region of the activation loop. The dichloro- and dimethoxy- substituted benzene resides in a hydrophobic region formed by Phe631, Met524, and multiple hydrophobic residues located on the beta sheet of the N-lobe including Val481. In addition to hydrophobic interactions, one methoxy group forms a hydrogen bond with the main chain NH of Asp630.

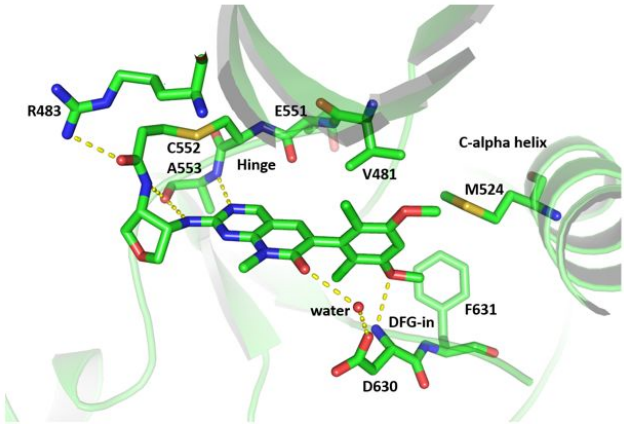

Figure 2. Co-crystal structure of compound **1** in complex with FGFR4 determined to 1.9 Å resolution. Compound **1** forms a covalent bond to Cys552 and two H-bonds with Ala553 in the hinge region of the ATP binding pocket. The dimethoxyphenyl group binds in a hydrophobic pocket and forms H-bond interactions with Asp630.

Structural alterations and a matched pair analysis with compound **1** furthered our understanding of structure-activity relationships (SAR). Covalency was critical for potency as well as selectivity, demonstrated by a comparison of **1** with its reversible propionamide analog **2**. Positioning of the acrylamide was impactful, and a reversal in the absolute configuration of the adjacent stereocenter, as shown in compound **3**, resulted in a significant loss in potency and selectivity. Covalent modifiers with increased cysteine reactivity such as vinylsulfonamide **5** led to erosion of selectivity without a gain in potency. The penta-substituted benzene in the hydrophobic back pocket of FGFR4 could be modified to maintain or attenuate potency and selectivity. Removal of either chloro or methoxy groups led to reduced potency. However, replacing either or both chlorines with fluorine resulted in similar levels of potency and selectivity.

The synthesis of compound **1** is shown in Scheme 1. Chloropyrimidine **11** was treated with methylamine to displace the chloride in quantitative yield. The methylamine adduct was then subjected to reduction with $LiAlH_4$ and oxidation with MnO_2 to furnish aldehyde **12** in 40% overall yield in two steps. Thermal condensation of **12** with **13** in the presence of K_2CO_3 provided **14** in 63% yield. Simultaneous oxidation and chlorination of **14** was achieved with SO_2Cl_2 in 70% yield. The sulfone moiety in **55** was converted to a chloride in sequential hydrolysis and chlorination steps with 79% overall yield. Coupling of **16** with amine **17** furnished **18** in 71% yield. Boc deprotection followed by acrylamide formation provided compound **1** in 65% yield over two steps.

Table 1. Kinase Inhibitory Activities of Compounds

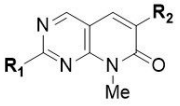

Compound	R_1	R_2	Enzymatic IC_{50} (nM)[a]		Cellular IC_{50} (nM)[b]		Compound	R_1	R_2	Enzymatic IC_{50} (nM)[a]		Cellular IC_{50} (nM)[b]	
			FGFR4	FGFR2[c]	FGFR4	FGFR2[c]				FGFR4	FGFR2[c]	FGFR4	FGFR2[c]
1			6.5	505	8.8	842	**6**			13	2156	29	3602
2		---	2340	394	2926	377	**7**	---		588	10000	685	5000
3		---	3161	776	2212	1219	**8**	---		10	5132	25	5000
4		---	73	247	35	359	**9**	---		4.1	672	11.4	1172
5		---	6	102	20	218	**10**	---		6.5	563	7.2	617

[a]Values determined using an Omnia® Kinase Assay at 250 uM ATP. [b] pFGFR4 and pFGFR2 formation in Huh7 and KATO cells, respectively. [c]Inhibition of FGFR2 phosphorylation was used as a surrogate for FGFR1 and FGFR3, as potencies against these off-targets were similar

Scheme 1. Synthesis of Compound **1**[a]

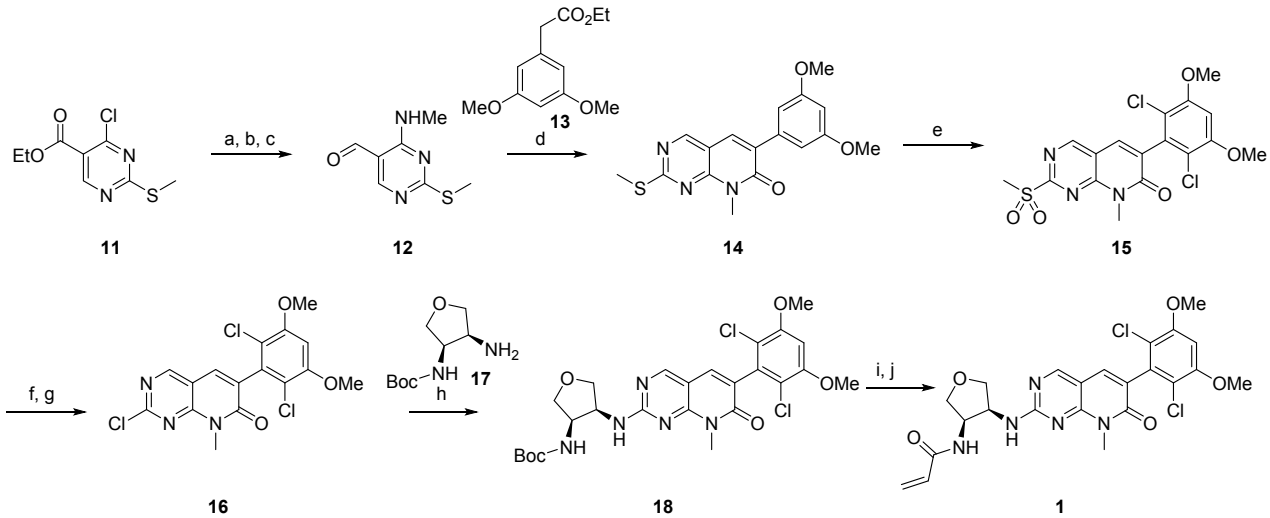

[a]Reagents and conditions: (a) $MeNH_2$, DCM, 0 °C, 30 min, 100%; (b) LiAlH4, THF, 15 min, 53%; (c) MnO_2, DCM, 24 h, 75%; (d) **10**, K_2CO_3, DMF, 110 °C, 4 h, 63%; (e) SO_2Cl_2, DCM, 0 °C, 30 min, 70%; (f) KOH, THF/H_2O (1:1), 0 °C , 4 h, 83%; (g) $POCl_3$, CH_3CN, 90 °C, 6 h, 95%; (h) 14, DIPEA, NMP, 90 °C, 2 h, 71%; (i) TFA, DCM, 2 h, 97%; (j) acryloyl chloride, DCM, DIPEA, -78 °C, 10 min, 67%.

Pharmacokinetic analysis of **1** revealed a high C_{max}, low clearance, and 20, 12, and 27% oral bioavailability in mouse, rat, and cyno, respectively (Table 2). Pharmacodynamic (PD) effects were studied by measuring target occupancy and

inhibition of pFGFR4 signaling in Huh7 tumor-bearing mice after single dose oral administration at 2.5, 10, 30 and 100 mg/kg. FGFR4 autophosphorylation, measured by Mesoscale Discovery (MSD) assays, was inhibited in a dose dependent manner over a time course of 1–8 hours. The degree of target occupancy, determined by ratio of unbound to total FGFR4, was in close correlation with inhibition of pFGFR4 signaling, with max inhibition observed at Cmax. Target occupancy >80% was sustained for approximately 10h after a single dose (Figure 3).

Table 2. Pharmacokinetics of Compound **1** in Mouse, Rat and Cynomolgus Monkey

Species	Mouse		Rat		Cyno	
Route	iv	po	iv	po	iv	po
Dose (mg/kg)	3	10	3	10	3	10
CL (mL/min/kg)	17.2		9.0		8.4	
V_{ss} (L/Kg)	0.63		0.30		1.1	
$T_{1/2}$(hr)	2.1	1.8	2.1	3.2	4.8	2.0
C_{max} (mg/mL)	6270	423	9130	588	5100	2820
AUC (ng*hr/mL)	2910	2960	5610	2230	6420	5660
%F		20		12		27

The anti-tumor activity of **1** was studied in two human tumor xenograft (HTX) models of HCC including an orthotopic model of (Hep3B) HCC and a subcutaneous model of sorafenib resistant Huh7 tumor growth, in SCID mice. In a Hep3B model, 100 mg/kg of inhibitor **1** administered PO daily resulted in tumor regression and sustained growth inhibition over 28 days (Figure 4). Sorafenib-resistant tumors were established by orally administering sorafenib to animals bearing Huh7 tumors, at a dose of 100 mg/kg twice daily for fourteen months until the tumors were completely resistant to treatment. After establishment of sorafenib-resistant Huh7 tumors, oral administration of **1** at 10, 30 and 100 mg/kg BID for 11 days resulted in dose-dependent growth inhibition of sorafenib-resistant tumors. Tumor regression was observed at 30 and 100 mg/kg, with % $\Delta T/\Delta C$ = -67% and -70% respectively ($p < 0.0001$). As expected, treatment with sorafenib at 100 mg/kg once daily did not provide any benefit (Figure 5).

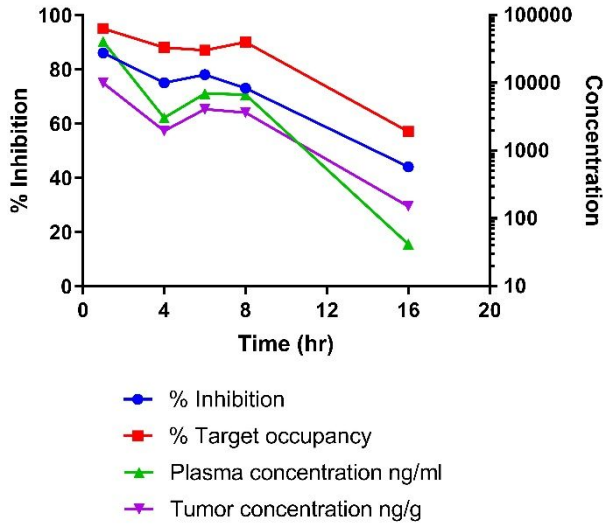

Figure 3. pFGFR4 inhibition and target occupancy as a function of time in Huh7 tumor-bearing SCID mice after a single oral administration (100 mpk) of **1**.

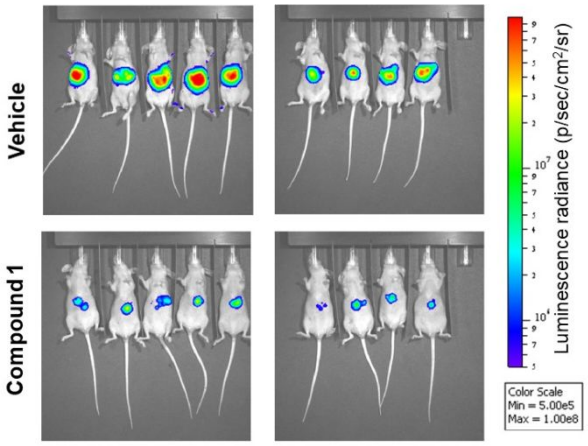

Figure 4. Antitumor activity of compound **1** (100 mg/kg BID) against orthotopic Hep3B human tumors in SCID mice, on day 28 of treatment.

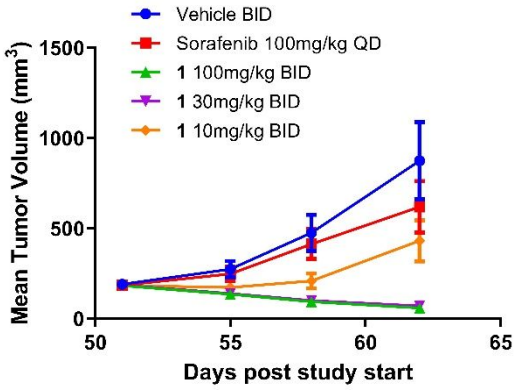

Figure 5. Antitumor activity of compound **1** against subcutaneous sorafenib resistant Huh7 human tumors in SCID mice.

In summary, a series of covalent and selective FGFR4 inhibitors were identified. Potent inhibition of FGFR4 phosphorylation was achieved enzymatically and in cells. Isoform and kinome selectivity were achieved, in part, through covalent modification of the unique Cys552, which was confirmed by X-ray crystallography. In addition, compound **1** achieved sufficient *in vivo* exposure to acheive high levels of FGFR4 occupancy and pFGFR4 inhibition, in tumor bearing mice. In orthotopic and sorafenib-resistant HCC HTX models, oral administration of **1** resulted in notable and sustained tumor regression. Collectively, these data support the potential utility of **1** for treatment of FGF19/FGFR4 driven diseases including sorafenib resistant HCC.

SUPPORTING INFORMATION

The Supporting Information is available free of charge on the ACS Publications website.

Synthetic procedures and analytical data of selected compounds, conditions for all biological assays, and X-ray crystallographic methods and statistics, kinome inhibition profiling, *in vivo* PK/PD protocols and tumor growth inhibition studies protocols. (PDF)

AUTHOR INFORMATION

Corresponding Author

* E-mail: ldagostino@celgene.com

Present Addresses

†If an author's address is different than the one given in the affiliation line, this information may be included here.

Author Contributions

The manuscript was written through contributions of all authors. All authors have given approval to the final version of the manuscript.

Notes

The authors declare no competing financial interest.

ABBREVIATIONS

FGFR, fibroblast growth factor receptor; FGF, fibroblast growth factor; DMPK, drug metabolism and pharmacokinetics; HCC, hepatocellular carcinoma; PK, pharmacokinetics; PD, pharmacodynamics; EU, European Union; anti-PD1, programmed cell death protein 1 antibody; KLB, cofactor β-klotho; DFG, Asp-Phe-Gly motif; Boc, tert-butyloxycarbonyl protecting group; DIPEA, N,N-diisopropylethylamine; NMP, N-methyl-2-pyrrolidone; TFA, trifluoroacetic acid; MSD, mesoscale discovery; cyno, cynomolgus monkey; CL, clearance; Vss, volume of distribution; $T_{1/2}$, half-life; Cmax, maximum serum concentration; AUC, area under the curve; %F, oral bioavailability; HTX, human tumor xenograft; QD, once a day; SCID, severe combined immunodeficiency.

REFERENCES

(1) Taylor, F.; Best, J.; Schotten, C.; Lohmann, G.; Gerken, G.; Dechêne, A. Tivantinib for the treatment of hepatocellular carcinoma. *Expert Opin. Pharmacother*. **2017**, *18*, 727−733.

(2) Bray F; Ferlay J; Soerjomataram I; Siegel RL; Torre LA; Jemal A. Global cancer statistics 2018: GLOBOCAN estimates of incidence and mortality worldwide for 36 cancers in 185 countries. *CA Cancer J Clin.* **2018**, *68*, 394–424.

(3) Jou, J. H.; Muir, A. J. Hepatocellular Carcinoma Surveillance. *Clin. Gastroenterol. and Hepatol.*, **2018**, *16*, 19-20.

(4) Llovet, J. M; Ricci, S.; Mazzaferro, V.; Hilgard, P.; Gane, E.; Blanc, J.-F.; de Oliveira, A. C.; Santoro, A.; Raoul, J.-L.; Forner, A.; Schwartz, M.; Porta, C.; Zeuzem, S. *et. al*. Sorafenib in Advanced Hepatocellular Carcinoma. *N. Engl. J. Med.*, **2008**, *359*, 378-390.

(5) Niu, L.; Liu, L.; Yang, S.; Ren, J.; Lai, P. B.; Chen, G. G. New insights into sorafenib resistance in hepatocellular carcinoma: Responsible mechanisms and promising strategies. *Biochim. Biophys. Acta, Rev. Cancer*, **2017**, *1868*, 564-570.

(6) Balogh, J.; Victor III, D.; Asham, E.; Burroughs, S.; Boktour, M.; Saharia, A.; Li, X.; Ghobrial, R.; Monsour Jr, H. Hepatocellular carcinoma: a review. *J. Hepatocell. Carcinoma*, 2016, 3, 41-53.

(7) Touat, M.; Ileana, E.; Postel-Vinay, S.; André, F.; Soria, J.-C. Targeting FGFR Signaling in Cancer. *Clin. Cancer Res.*, **2015**, *21*, 2684-2694.

(8) Desnoyers, L. R.; Pai, R.; Ferrando, R. E.; Hötzel, K.; Le, T.; Ross, J.; Carano, R.; D'Souza, A.; Qing, J.; Mohtashemi, I.; Ashkenazi, A.; French, D. M. Targeting FGF19 inhibits tumor growth in colon cancer xenograft and FGF19 transgenic hepatocellular carcinoma models. *Oncogene*, **2008**, *27*, 85-97.

(9) French, D. M.; Lin, D. C.; Wang, M.; Adams, C.; Shek, T.; Hotzel, K.; Bolon, B.; Ferrando, R.; Blackmore, C.; Schroeder, K.; Rodriguez, L. A.; Hristopoulos, M.; Venook, R.; Ashkenazi, A.; Desnoyers, L. R. Targeting FGFR4 Inhibits Hepatocellular Carcinoma in Preclinical Mouse Models. *PLoS One*, **2012**, *7*, e36713.

(10) Sawey, E. T.; Chanrion, M.; Cai, C.; Wu, G.; Zhang, J.; Zender, L.; Zhao, A.; Busuttil, R. W.; Yee, H.; Stein, L.; French, D. M.; Finn, R. S.; Lowe, S. W.; Powers, S. Identification of a Therapeutic Strategy Targeting Amplified FGF19 in Liver Cancer by Oncogenomic Screening. *Cancer Cell*, **2011**, *19*, 347-358.

(11) Lu, X.; Chen, H.; Patterson, A. V.; Smaill, J. B.; Ding, K. Fibroblast Growth Factor Receptor 4 (FGFR4) Selective Inhibitors as Hepatocellular Carcinoma Therapy: Advances and Prospects. *J. Med. Chem.*, **2019**, *62*, 2905–2915.

(12) Kim, R. D.; Sarker, D.; Meyer, T.; Yau, T.; Macarulla, T.; Park, J-W.; Choo, S. P.; Hollebecque, A.; Sung, M. W.; Lim, H-Y. ; Mazzaferro, V.; Trojan, J.; Zhu, A. X.; Yoon, J-H.; Sharma, S.; Lin, Z-Z.; Chan, S. L.; Faivre, S.; Feun, L. G.; Yen, C-J.; Dufour, J-F.; Palmer, D. H.; Llovet, J. M.; Manoogian, M.; Tugnait, M.; Stransky, N.; Hagel, M.; Kohl, N. E.; Lengauer, C.; Sherwin, C. A.; Schmidt-Kittler, O.; Hoeflich, K. P.; Shi, H.; Wolf, B. B.; Kang, Y-K. First-in-Human Phase I Study of Fisogatinib (BLU-554) Validates Aberrant FGF19 Signaling as a Driver Event in Hepatocellular Carcinoma. *Cancer Discovery*, **2019**, *9*, 1696-1707.

(13) Juswinder, S.; Petter, R. C.; Baillie, T. A.; Adrian, W. The resurgence of covalent drugs. *Nat. Rev. Drug Discovery*, **2011**, *10*, 307-317.

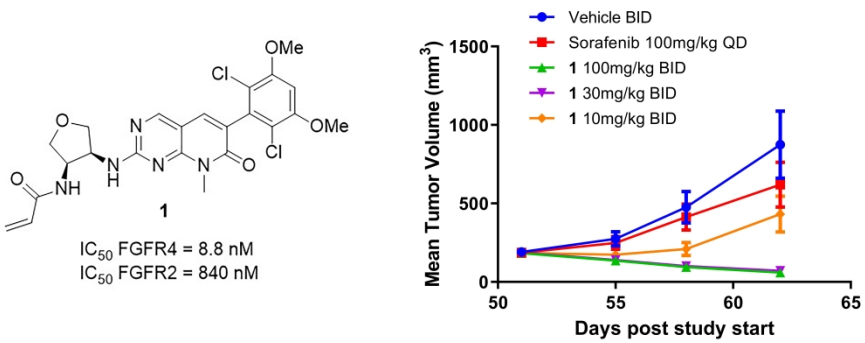

215x78mm (1200 x 1200 DPI)